

# Clustering of integrin $\alpha 5$ at the lateral membrane restores epithelial polarity in invasive colorectal cancer cells

Alina Starchenko<sup>a</sup>, Ramona Graves-Deal<sup>b</sup>, Yu-Ping Yang<sup>b</sup>, Cunxi Li<sup>b</sup>, Roy Zent<sup>b</sup>, Bhuminder Singh<sup>b</sup>, and Robert J. Coffey<sup>b,c,\*</sup>

<sup>a</sup>Department of Cell and Developmental Biology, Vanderbilt University, Nashville, TN 37232; <sup>b</sup>Department of Medicine, Vanderbilt University Medical Center, Nashville, TN 37232; <sup>c</sup>Veterans Affairs Medical Center, Nashville, TN 37212

**ABSTRACT** Apicobasolateral polarity is a fundamental property of epithelial cells, and its loss is a hallmark of cancer. Integrin-mediated contact with the extracellular matrix defines the basal surface, setting in motion E-cadherin-mediated cell–cell contact, which establishes apicobasolateral polarity. Role(s) for lateral integrins in this polarization process and the consequences of their disruption are incompletely understood. We show that addition of an integrin  $\beta 1$ -activating monoclonal antibody, P4G11, to invasive colorectal cancer cells in three-dimensional type 1 collagen reverts the invasive phenotype and restores apicobasolateral polarity. P4G11 induces clustering of integrin  $\alpha 5\beta 1$  at lateral, intercellular surfaces. This leads to deposition and polymerization of fibronectin and recruitment of paxillin to sites of lateral integrin  $\alpha 5\beta 1$  clustering and is followed by tight junction formation, as determined by ZO-1 localization. Inducible elimination of integrin  $\alpha 5$  abrogates the epithelial-organizing effects of P4G11. In addition, polymerization of fibronectin is required for the effects of P4G11, and addition of polymerized superfibronectin is sufficient to induce tight junction formation and apicobasolateral polarization. In the normal human colon, we show that integrin  $\alpha 5$  localizes to the lateral membrane of terminally differentiated colonocytes and that integrin  $\alpha 5$  staining may be reduced in colorectal cancer. Thus we propose a novel role for integrin  $\alpha 5\beta 1$  in regulating epithelial morphogenesis.

## Monitoring Editor

Jean E. Schwarzbauer  
Princeton University

Received: Dec 15, 2016

Revised: Mar 20, 2017

Accepted: Mar 21, 2017

## INTRODUCTION

Polarized epithelial cells line the boundary between the interior of an organism and its external environment. The ability of the cells to distinguish between their basolateral (internal) and apical (external) sides allows for regulated exchange of nutrients and their byproducts. Integrin engagement of extracellular matrix (ECM) ligands

defines the basal cell surface and appears to be the first step in apicobasolateral polarization (Ojakian and Schwimmer, 1988; Yeaman *et al.*, 1999; Yu *et al.*, 2005; Akhtar and Streuli, 2013).

Studies *in vivo* and *in vitro* show that integrin  $\beta 1$  is required for epithelial morphogenesis (Jones *et al.*, 2005; Chen and Krasnow, 2012). Apart from its role in orienting the apical surface (O'Brien *et al.*, 2001), integrin  $\beta 1$  signaling is believed to provide a cue for the recruitment of E-cadherin to nascent cell–cell contacts, stabilizing the extending lateral membrane and culminating in formation of tight junctions (Schreider *et al.*, 2002). *In vitro*, blockade or knockdown of integrin  $\beta 1$  leads to cytoskeletal disorganization and loss of apicobasolateral polarity (Akhtar and Streuli, 2013). *In vivo*, elimination of integrin  $\beta 1$  in the gut leads to defects in epithelial differentiation and proliferation, resulting in a disorganized tissue and postnatal lethality (Jones *et al.*, 2005). The mechanisms by which modulation of integrin  $\beta 1$  signaling contributes to epithelial morphogenesis are incompletely understood.

This article was published online ahead of print in MBoC in Press (<http://www.molbiolcell.org/cgi/doi/10.1091/mbc.E16-12-0852>) on March 29, 2017.

\*Address correspondence to: Robert J. Coffey ([robert.coffey@vanderbilt.edu](mailto:robert.coffey@vanderbilt.edu)).

Abbreviations used: AJ, adherens junction; CC, cystic colonies; CRC, colorectal cancer; ECM, extracellular matrix; EGFR, EGF receptor; FN, fibronectin; ITG, integrin; MMC, monomeric collagen; SC, spiky colonies; TJ, tight junction.

© 2017 Starchenko *et al.* This article is distributed by The American Society for Cell Biology under license from the author(s). Two months after publication it is available to the public under an Attribution–Noncommercial–Share Alike 3.0 Unported Creative Commons License (<http://creativecommons.org/licenses/by-nc-sa/3.0>).

“ASCB®,” “The American Society for Cell Biology®,” and “Molecular Biology of the Cell®” are registered trademarks of The American Society for Cell Biology.

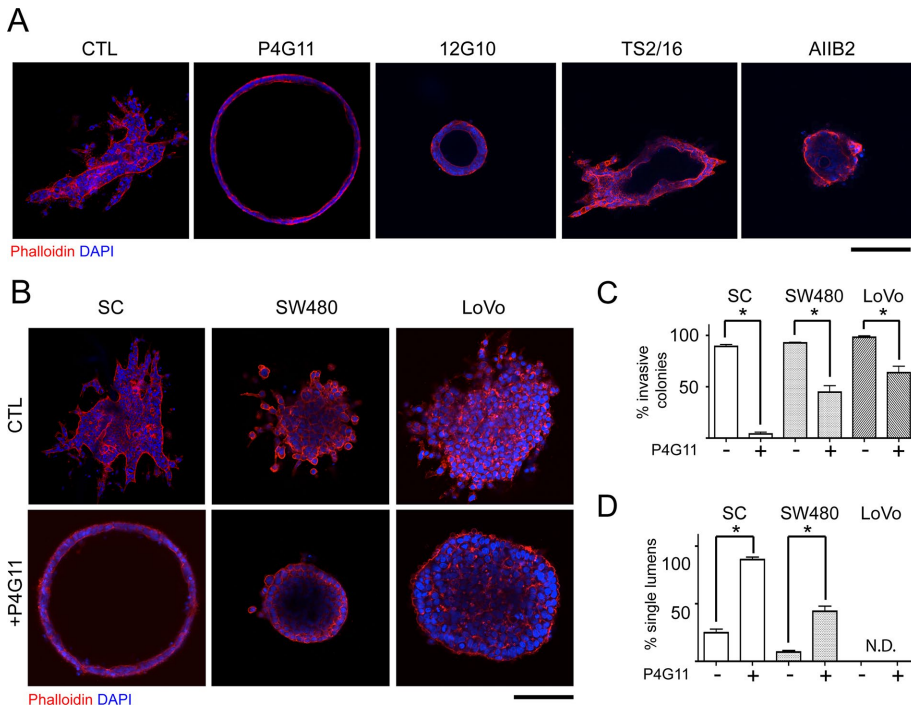


**FIGURE 1:** The integrin  $\beta 1$ -activating mAb P4G11 abrogates the invasive phenotype in CRC cells in 3D. (A) SC cells were plated in 3D type 1 collagen as single cells in the presence or absence of integrin  $\beta 1$  mAbs (10  $\mu\text{g}/\text{ml}$ ) as indicated. The medium was replaced every 2–3 d until day 15, when colonies were fixed and stained with phalloidin (red) and DAPI (blue). Scale bar, 100  $\mu\text{m}$ . (B) SC, SW480, and LoVo cells were plated as single cells in type 1 collagen, and medium was replaced every 2–3 d. At day 8, P4G11 (10  $\mu\text{g}/\text{ml}$ ) was added, and medium was again changed every 2–3 d until day 15, when colonies were processed as in A. Scale bar, 100  $\mu\text{m}$ . (C) Quantification of invasive phenotype of colonies growing in type 1 collagen in the presence or absence of P4G11 (mean  $\pm$  SEM; >400 colonies from three separate replicates). (D) Quantification of percentage of colonies forming a single central lumen in B (mean  $\pm$  SEM; >400 colonies in each of three separate replicates). N.D., not detected. Asterisks signify statistical significance with  $p < 0.05$ .

Integrin  $\beta 1$  heterodimerizes with one of 12 different  $\alpha$  subunits to form a functional receptor (Campbell and Humphries, 2011). The diverse developmental phenotypes in global *Itgb1*-knockout mice suggest that these heterodimers have distinct functions (Bouvard *et al.*, 2013). As human colorectal cancer (CRC) Caco-2 cells differentiate in vitro, they undergo a switch from integrin  $\alpha 2$  expression to integrin  $\alpha 3$  and  $\alpha 5$  expression (Halbleib *et al.*, 2007). Of interest, levels of both integrin  $\alpha 3$  and  $\alpha 5$  are reduced during human CRC progression (Stallmach *et al.*, 1992). The importance of integrin  $\alpha 5$  in epithelial morphogenesis in vivo is further noted in systems that rely on branching morphogenesis in a fibronectin-dependent manner, although a mechanistic explanation for this is lacking (Williams *et al.*, 2008). The contribution of  $\alpha 5$  subunits to epithelial polarity, particularly in the colon, also remains largely unexplored.

Here we examine the effect of integrin  $\beta 1$ -activating monoclonal antibodies (mAbs) on CRC cells, which exhibit an invasive phenotype when cultured in three-dimensional (3D) type 1 collagen. We discovered that the integrin  $\beta 1$ -activating mAb P4G11 blocks the invasive phenotype and restores apicobasolateral polarity. We performed a detailed characterization of how P4G11 achieves this remarkable reversion. By stabilizing integrin  $\beta 1$  at the lateral membrane, P4G11 induces clustering of integrin  $\alpha 5$ , which in turn leads to lateral deposition and polymerization of fibronectin. Both integrin  $\alpha 5$  and polymerized fibronectin are required for the epithelial reorganizing effect of P4G11. Moreover, we detect integrin  $\alpha 5$  and

fibronectin at the lateral membrane of terminally differentiated colonocytes in vivo in the human colon, suggesting the possible physiological relevance of these findings.

## RESULTS

### Integrin $\beta 1$ -activating antibody P4G11 reduces invasion and restores apicobasolateral polarity in invasive CRC cells

Integrin  $\beta 1$  and type 1 collagen are reported to be important mediators of polarity in 3D (Howlett *et al.*, 1995; Yu *et al.*, 2005; Park *et al.*, 2006). We sought to determine whether altering integrin  $\beta 1$  function in invasive CRC cells cultured in type 1 collagen might restore a more normal epithelial architecture. We recently developed a 3D system ideally suited to address this possibility (Li *et al.*, 2014, 2017). By placing single cells from a human CRC cell line, HCA-7, in 3D type 1 collagen, we derived cell lines with two distinct morphological and functional properties: single-layered polarized cysts, designated cystic colonies (CC), and solid, spiky masses, designated spiky colonies (SC). On subcutaneous injection into athymic nude mice, CC form indolent, well-differentiated tumors, whereas SC form locally invasive tumors (Li *et al.*, 2014). To assess whether integrin  $\beta 1$  activation might confer a less invasive morphology on SC, we plated single SC cells into 3D type 1 collagen and treated them with a panel of integrin  $\beta 1$  function-altering mAbs on days 1–15 (Byron *et al.*, 2009). SC colonies treated with P4G11 no longer formed invasive protrusions but

instead formed unilamellar cysts containing a single central lumen (Figure 1A). Although treatment with another integrin  $\beta 1$ -activating mAb, 12G10, eliminated invasion, and colonies exhibited lumen formation, the cells surrounding the lumen were multilayered, and many colonies formed several lumens. A third integrin  $\beta 1$ -activating mAb, TS2/16, did not alter colony morphology, even at significantly higher concentrations (unpublished data). On addition of an integrin  $\beta 1$ -blocking mAb, AIB2, SC colonies appeared as solid masses of cells. Thus, altering integrin  $\beta 1$  activity shows profound effects on colony morphogenesis in 3D.

We next examined whether P4G11 might restore epithelial polarity in two other CRC cell lines (SW480 and LoVo) that exhibit an invasive morphology when cultured in 3D type 1 collagen. In this experiment, we also tested whether P4G11 might restore a more normal epithelial architecture to established colonies, and so P4G11 was added after the colonies had fully formed. SC, SW480, and LoVo cells were plated as single cells into type 1 collagen and allowed to grow for 8 d, at which time colonies were treated with P4G11 until day 15. Invasion was markedly reduced in all three lines (Figure 1, B and C). Lumen formation was observed in SC and SW480 colonies but not in LoVo colonies (Figure 1, B and D). Even though P4G11 was not administered to these cells until invasive colonies were fully formed, SC colonies still reverted to single-layered cysts with a central lumen, as occurred when P4G11 was added at the time of plating.

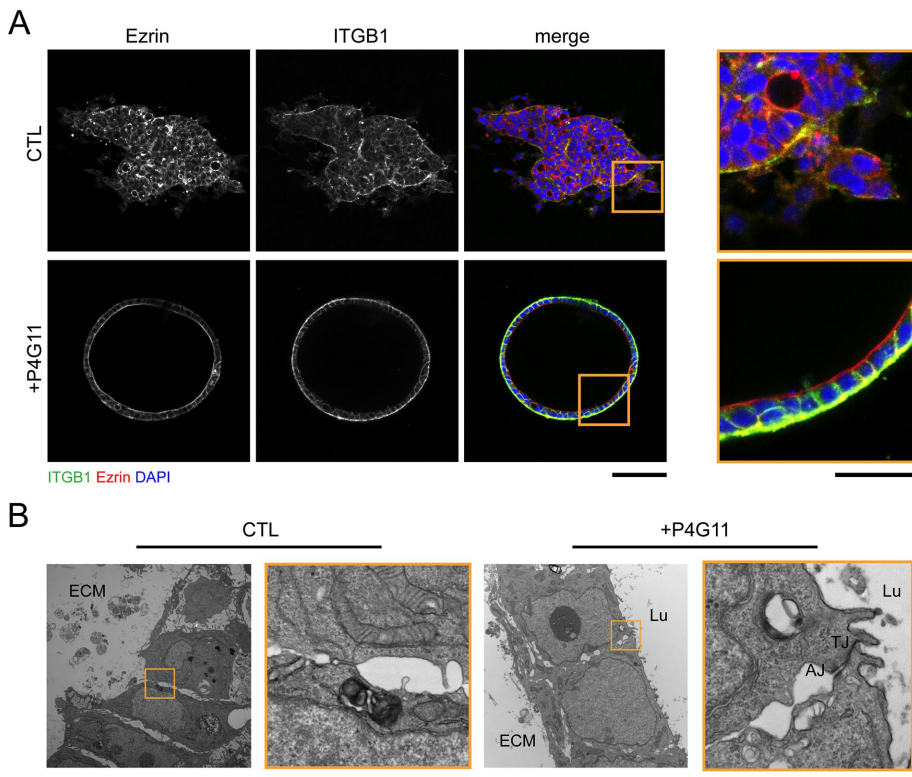


**FIGURE 2:** P4G11 restores apicobasolateral polarity and epithelial cell–cell junctions in 3D. (A) SC cells were plated as single cells in type 1 collagen, and medium was replaced every 2–3 d. At day 8, P4G11 (10  $\mu\text{g}/\text{ml}$ ) was added, and medium was again changed every 2–3 d until day 15, when colonies were fixed and stained with antibodies against integrin  $\beta 1$  (green), ezrin (red), and DAPI (blue). Representative confocal cross section through the equatorial plane of SC colonies. Scale bar, 100  $\mu\text{m}$  (main images), 25  $\mu\text{m}$  (insets). (B) Representative TEM images of SC colonies treated with P4G11. Highlighted sections are displayed at higher magnification on the right of each morphology. AJ, adherens junction; ECM, extracellular matrix; Lu, lumen; TJ, tight junction. Note the appearance of AJ and TJ in the magnified region in SC colonies treated with P4G11. Scale bars, 5  $\mu\text{m}$  (main images), 2.5  $\mu\text{m}$  (insets).

Having established that epithelial architecture is restored by P4G11, we examined its morphological effects on SC in more detail. Immunofluorescence analysis, using ezrin as an apical marker and integrin  $\beta 1$  as a basolateral marker, showed that cells in P4G11-treated SC colonies exhibit apicobasolateral polarity (Figure 2A). Using transmission electron microscopy (TEM), we determined that P4G11 treatment induces formation of tight junctions and adherens junctions beneath the apical surface (Figure 2B). To better track P4G11-mediated effects, we adopted a two-dimensional (2D) system that was amenable to high-magnification microscopy. We treated SW480 cells plated on monomeric collagen (MMC)-coated coverglass and found that P4G11 restored tight junction formation and polarity in these cells under these conditions (Supplemental Figure S2, A–D). We used a Transwell filter diffusion assay to test whether the ZO-1 localization to a tight junction-like structure corresponds to a functional decrease in paracellular permeability. P4G11 treatment of SW480 cells cultured on Transwell filters slows the rate of diffusion of 70-kDa fluorescein isothiocyanate (FITC)-dextran across the filter (Supplemental Figure S2E). Thus we conclude that P4G11-mediated activation of integrin  $\beta 1$  restores epithelial junctions and features of apicobasolateral polarity to invasive CRC cells.

### P4G11 induces clustering of integrin $\beta 1$

To define the mechanism by which P4G11 induced these phenotypic effects, we first confirmed that P4G11 bound human integrin  $\beta 1$ , using a mouse cell line stably expressing human integrin  $\beta 1$  (Supplemental Figure S1A). Treatment of cells with manganese ( $\text{Mn}^{2+}$ ) increases the amount of active integrin  $\beta 1$  at the cell surface (Dransfield *et al.*, 1992). To confirm that P4G11 recognizes this active form of integrin  $\beta 1$ , we treated cells with  $\text{Mn}^{2+}$  and noted that this increased P4G11 binding (Supplemental Figure S1B). P4G11 and 12G10 both increased the adhesion rate of suspended cells to a collagen substrate. Further, P4G11 and 12G10 both increased FAK phosphorylation (Supplemental Figure S1, C and D). Thus we conclude that P4G11 activates a population of integrin  $\beta 1$ .

Both P4G11 and 12G10 target ligand-induced binding sites (LIBS) on integrin  $\beta 1$ , but the effects of these antibodies on live cells are poorly understood (Humphries *et al.*, 2005; Araki *et al.*, 2009). This led us to compare their effects on integrin  $\beta 1$  localization and stability (Figure 3). We visualized 12G10 and P4G11 localization in SC after 15 d of exposure to these antibodies in 3D. P4G11 binding extended throughout the basolateral surface of a given cell in the cyst, whereas the 12G10 signal was primarily basal (Figure 3A). We used confocal microscopy to compare P4G11 and 12G10 internalization and their effect on integrin  $\beta 1$  degradation. SC cells plated in two dimensions on MMC-coated coverglass were costained with the lysosomal marker LysoTracker and fluorophore-labeled P4G11 or 12G10. A substantial amount of P4G11 was bound at the lateral cell–cell interface at baseline and was still retained there at 24 h. The 12G10 was detected at the cell surface initially but appeared to be internalized and colocalized with LysoTracker at 24 h (Figure 3B). Immunoblot analysis of total integrin  $\beta 1$  levels with increasing concentrations of 12G10 or P4G11 for 24 h on MMC-coated filters showed increased integrin  $\beta 1$  protein degradation in 12G10-treated cells (Figure 3C) compared with P4G11-treated cells. Loss of surface integrin  $\beta 1$  after 24 h of 12G10 treatment was further confirmed through cell-surface biotinylation (Figure 3D). From these studies, we conclude that P4G11 binds a population of integrin  $\beta 1$  that is retained at the cell surface.

Integrin function-altering mAbs are bivalent and can cross-link integrin  $\beta 1$  in live cells in a manner that mimics cell-driven cluster formation (Kornberg *et al.*, 1991; Jewell *et al.*, 1995), which is a significant step in the formation of mature adhesion complexes and is critical for certain signaling events (Hato *et al.*, 1998; Calderwood *et al.*, 2000). To determine whether P4G11 mediates its effects through induction of integrin  $\beta 1$  clustering at the cell surface, we digested P4G11 into light/heavy chain F(ab)' fragments, which were subsequently conjugated to a fluorophore. P4G11 F(ab)' is capable of binding to integrin  $\beta 1$  but is not retained at the lateral cell surface (Figure 4, A and C). Addition of an antibody against mouse heavy and

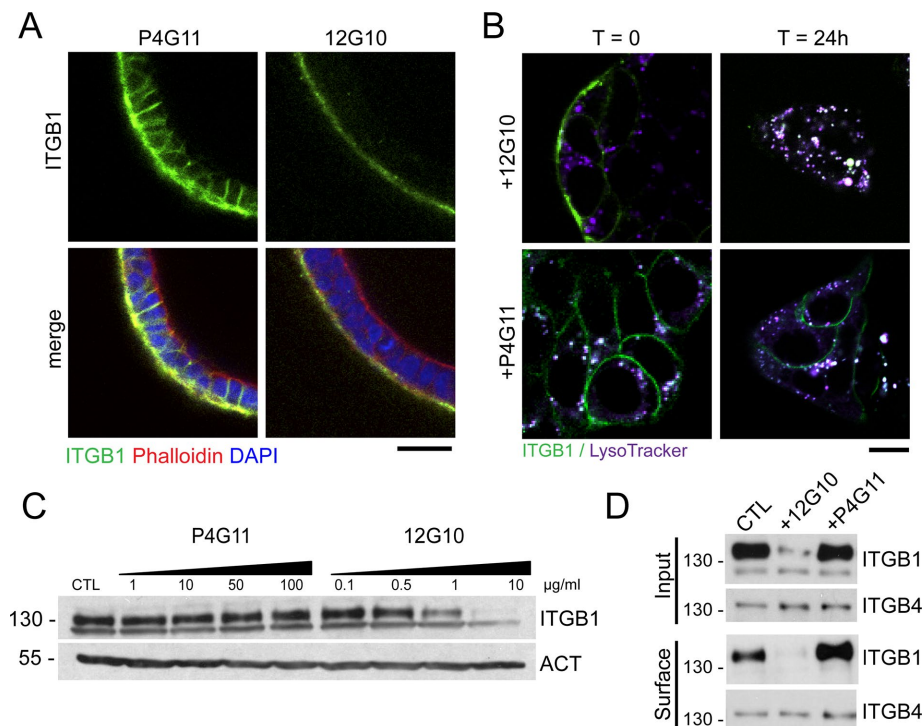


**FIGURE 3:** Differential processing of integrin  $\beta 1$  after treatment with two integrin  $\beta 1$ -activating mAbs. (A) Representative confocal images of SC colonies grown as in Figure 1A, fixed, and stained with DAPI (blue), phalloidin (red), and anti-Ms-488 (green) to determine localization of integrin  $\beta 1$ -bound P4G11 or 12G10 after treatment with antibody on days 1–15. Scale bar, 25  $\mu\text{m}$ . (B) Representative confocal image of SC grown on MMC-coated coverglass for 48 h and stained with LysoTracker-FarRed (LysoTracker) before 24 h of treatment with primary labeled P4G11 or 12G10. Initial and final localizations of the antibodies show different patterns in the cells, with substantial P4G11 remaining at the cell/cell surface and 12G10 being largely internalized and colocalized with LysoTracker-positive vesicles. Scale bar, 10  $\mu\text{m}$ . (C) SC cells grown on MMC-coated Transwell filters were treated with different concentrations of P4G11 or 12G10 for 24 h. The cells were examined by immunoblot analysis with antibodies to integrin  $\beta 1$  and phalloidin. Treatment of cells with 12G10 caused decreased cellular levels of integrin  $\beta 1$  at highest concentrations (1 and 10  $\mu\text{g}/\text{ml}$ ). Data are from one of at least three similar experiments with independent SC preparations. (D) Surface levels of integrin  $\beta 1$  in SC cells grown on MMC-coated Transwell filters treated with 12G10 or P4G11 (10  $\mu\text{g}/\text{ml}$ ) for 24 h were analyzed using cell-surface biotinylation and streptavidin immunoprecipitation, followed by immunoblot analysis with antibodies against integrin  $\beta 1$  and integrin  $\beta 4$  as a control.

light chain should rescue bivalency of P4G11 F(ab)' and, as expected, restores retention of cell-surface integrin  $\beta 1$  (Figure 4C). To ascertain whether the ability to cluster integrin  $\beta 1$  is necessary for P4G11 to rescue an epithelial morphology in 3D, we treated SC with P4G11 F(ab)', as well as with a combination of P4G11 F(ab)' and anti-mouse H+L. We found that loss of bivalency blocked the ability of P4G11 to reduce invasion in SC (Figure 4, A and B). Rescue of bivalency through addition of the anti-mouse secondary antibody restored the ability of P4G11 F(ab)' to convert SC to a cystic morphology (Figure 4, A and B) and induced basolateral retention of the F(ab)' fragment (Figure 4A, inset). Taken together, these results indicate that P4G11 bivalency is necessary for its ability to restore apicobasolateral polarity and strongly suggest that integrin  $\beta 1$  clustering at the cell surface drives this P4G11-induced phenotypic switch.

#### P4G11 treatment results in lateral clustering of integrin $\alpha 5$

Studies were next directed to determine which  $\alpha$  subunit was partnering with integrin  $\beta 1$  at the lateral membrane on P4G11 exposure. Integrin  $\alpha 5$  was a prime candidate because integrin  $\alpha 5$  expression correlates with a more differentiated state for CRC cells (Stallmach

et al., 1992; Halbleib et al., 2007). To determine whether integrin  $\alpha 5$  levels correlate with a differentiated cyst morphology in our CC and SC system, we compared levels of various integrin subunits by immunoblotting. Of the integrin subunits tested, only integrin  $\alpha 5$  protein levels were different and higher in CC than SC. However, treatment of SC with P4G11 did not increase integrin  $\alpha 5$  protein levels (Figure 5A). Because recycling and surface retention of integrins are key regulators of integrin signaling, we next asked whether P4G11 alters integrin  $\alpha 5$  surface distribution in SC. We grew SC cells on MMC-coated Transwell filters for 5 d, treated them with 10  $\mu\text{g}/\text{ml}$  P4G11 on days 5–6, and compared them with CC cells grown for 6 d on MMC-coated Transwell filters. We used confocal microscopy to generate an XZ-plane reconstruction through the cell to examine basolateral integrin distribution. We noted higher levels of membrane integrin  $\alpha 5$  staining in CC than SC and an increase in integrin  $\alpha 5$  staining at the lateral membrane after P4G11 treatment (Figure 5B). We did not note obvious changes in lateral integrin  $\beta 1$  staining (Figure 5B). We treated SC cells grown on MMC-coated Transwell filters with P4G11 over periods of time ranging from 30 min to 24 h and noted a gradual increase in surface integrin  $\alpha 5$  at the lateral cell membranes (Figure 5C). Using confocal microscopy, we determined that increased integrin  $\alpha 5$  staining was primarily lateral and brightest in the subapical region (Figure 5B). To determine whether this relocalization was selective for integrin  $\alpha 5/\beta 1$ , we compared it to the distribution of integrin  $\alpha 2$  (Figure 5D), another integrin  $\beta 1$  binding partner. We detected integrin  $\alpha 2$  along the entire basolateral membrane of SC cells with or without P4G11 treatment. The effect of P4G11 appeared to be selective for integrin  $\alpha 5$ , as it did not alter the overall distribution of the highly recycled transferrin receptor (Figure 5E). Next we used cell-surface biotinylation to confirm a selective increase in surface integrin  $\alpha 5$  in response to P4G11 treatment. SC colonies (treated with or without P4G11 overnight) were labeled with cell-impermeable biotin at 4°C. Cells were then lysed and subjected to streptavidin pull down to isolate surface proteins, followed by immunoblotting for integrins  $\alpha 5$ ,  $\beta 1$ , and  $\alpha 2$  (Figure 5, F and G). Integrin  $\alpha 5$  showed the most significant increase in surface levels after P4G11 treatment, whereas integrin  $\beta 1$  surface levels increased slightly and integrin  $\alpha 2$  surface levels were unchanged. Total cellular levels for all three proteins were unperturbed after P4G11 treatment. These data are recapitulated in 3D type 1 collagen (Figure 5, H and I). Taken together, these data suggest that P4G11 selectively increases levels of integrin  $\alpha 5/\beta 1$  at the lateral cell surface of SC.

#### Integrin $\alpha 5$ is necessary for apicobasolateral polarity in CRC cells

Given the dramatic difference in integrin  $\alpha 5$  membrane localization, we sought to examine directly its contribution to the

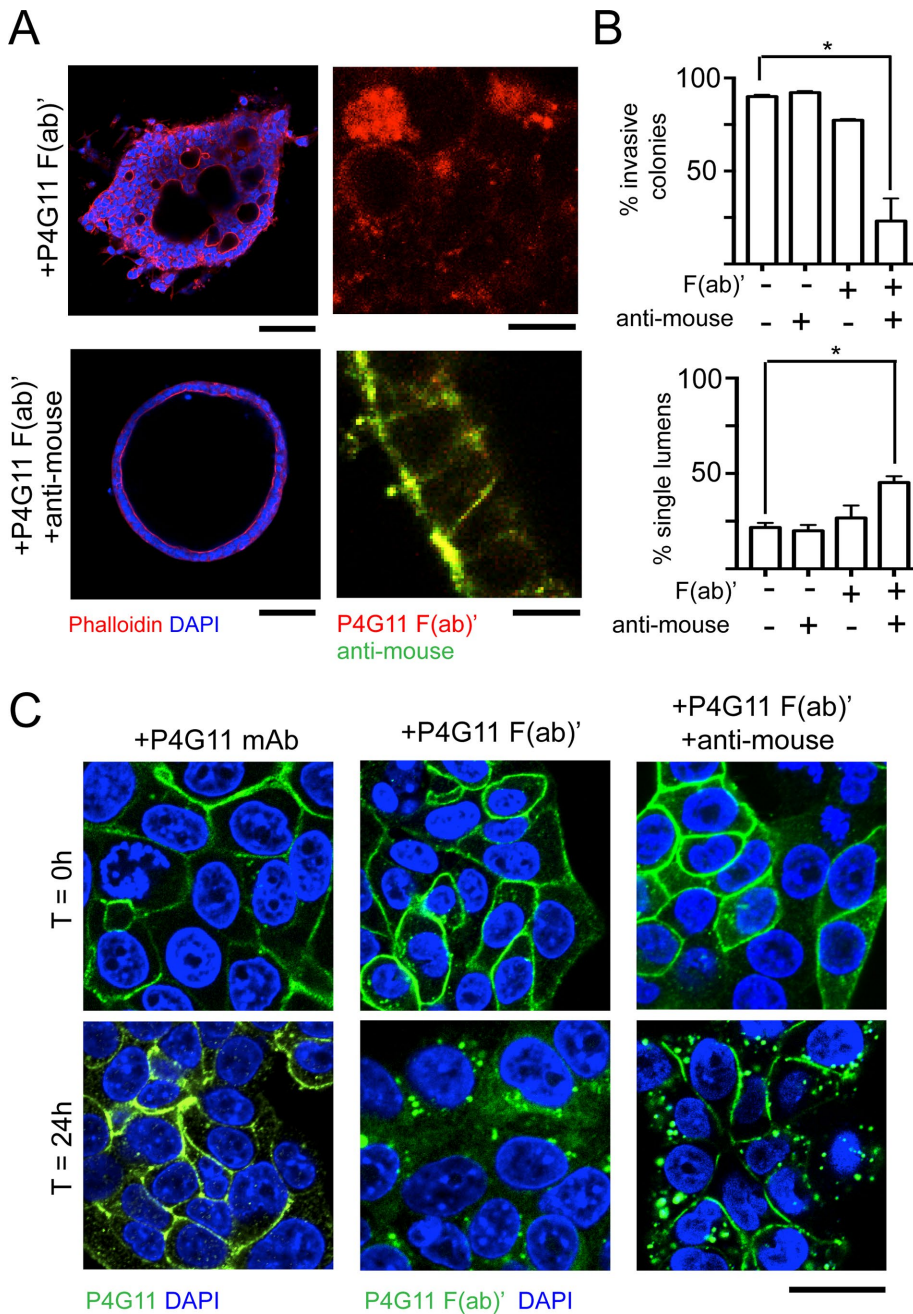


**FIGURE 4:** P4G11 clustering of integrin  $\beta 1$  is necessary for rescue of epithelial cyst architecture in SC cells grown in 3D type 1 collagen. (A) Representative confocal image of SC grown as in Figure 1A. At day 1, P4G11 f(ab)<sup>'</sup>-dy594 fragment at 10  $\mu\text{g}/\text{ml}$  in the presence or absence of a 488-conjugated anti-mouse secondary antibody. Colonies were grown until day 15, fixed, and stained with phalloidin (red) and DAPI (blue). Scale bar, 100  $\mu\text{m}$ . Inset, localization of F(ab)<sup>'</sup>-dy594 alone (red) or in the presence of anti-Ms (green). Scale bar, 10  $\mu\text{m}$ . (B) Quantification of the percentage of colonies exhibiting an invasive morphology, as well as a single lumen, with F(ab)<sup>'</sup>-dy594 fragment and with anti-Ms rescue (mean  $\pm$  SEM; >400 colonies from three separate replicates). (C) Representative confocal image through the midline of SC grown on MMC-coated coverglass and treated with 10  $\mu\text{g}/\text{ml}$  P4G11 mAb, F(ab)<sup>'</sup>-dy594, or F(ab)<sup>'</sup> with anti-mouse (H+L) chain antibody at 4°C (time 0). Cells were then incubated at 37°C for 24 h. Shown are cells treated at  $T = 0$  and 24 h. Note long-term membrane retention of F(ab)<sup>'</sup>-dy594 in the presence of anti-mouse secondary antibody. Scale bar, 20  $\mu\text{m}$ . Asterisks signify statistical significance with  $p < 0.05$ .

P4G11-mediated reorganization process. To this end, we generated a doxycycline (Dox)-inducible integrin  $\alpha 5$ -knockout system in which an anti-integrin  $\alpha 5$  short hairpin RNA (shRNA) was induced

upon addition of Dox. To lower the likelihood of nonspecific observations, we compared the phenotypes of two shRNA constructs, sh1 and sh3, which target different portions of the integrin  $\alpha 5$  mRNA. SC (SC-A5sh1) and SW480 (SW480-A5sh1) cells expressing both constructs were generated, and the ability of Dox to induce silencing of integrin  $\alpha 5$  was confirmed (Figure 6A and Supplemental Figure S3A). We did not observe any obvious compensatory changes in levels of either integrin  $\beta 1$  or integrin  $\alpha 2$ , despite having to treat with Dox for 4 d before plating due to the long half-life of integrin  $\alpha 5$  (Figure 6A and Supplemental Figure S3A). SC-A5sh1 and SW480-A5sh1 cells were grown in 3D type 1 collagen for 15 d in the presence of Dox to determine the contribution of integrin  $\alpha 5$  to cell growth and survival in 3D. Silencing integrin  $\alpha 5$  resulted in a 70% reduction in SC colony number (unpublished data). Cells that survived retained low but detectable integrin  $\alpha 5$  (Supplemental Figure S3A), complicating the analysis of SC in this assay. Thus, in subsequent experiments, we focused on SW480 cells; however, all of the trends noted in SW480 were also observed in SC (Supplemental Figure S3, A and B).

We hypothesized that the P4G11-induced epithelial reorganization requires integrin  $\alpha 5$ . To test this, we examined colony morphology after P4G11 treatment in cells in which integrin  $\alpha 5$  expression was silenced. We found that A5sh1- and A5sh3-expressing cells, in the absence of Dox, respond to P4G11-like parental cells (Figure 6, B and C). In marked contrast, when integrin  $\alpha 5$  was depleted with Dox-induced shRNA A5sh1 or A5sh3, we did not see a reduction in invasion after P4G11 treatment (Figure 6, B and C). To better determine whether integrin  $\alpha 5$  is required for cell polarity and tight junction formation in response to P4G11, we treated SW480-A5sh1 cells grown on MMC-coated coverglass with P4G11 in the presence or the absence of Dox. We examined the distribution of ZO-1, a marker of tight junctions, after 24-h exposure to P4G11. We found that P4G11-treated SW480 cells exhibited some polarity in the presence of integrin  $\alpha 5$ , with well-formed tight junctions and a general increase in lateral cell-cell interaction (Figure 6, D–F). When integrin  $\alpha 5$  was depleted by A5sh1, however, this polarization was disrupted in both P4G11-treated and -untreated cells (Figure 6, D and F). SW480 cells expressing integrin  $\alpha 5$  A5sh3 mirror these phenotypes (unpublished data). These data suggest that integrin  $\alpha 5$  is necessary for P4G11-mediated tight junction formation and epithelial reorganization.

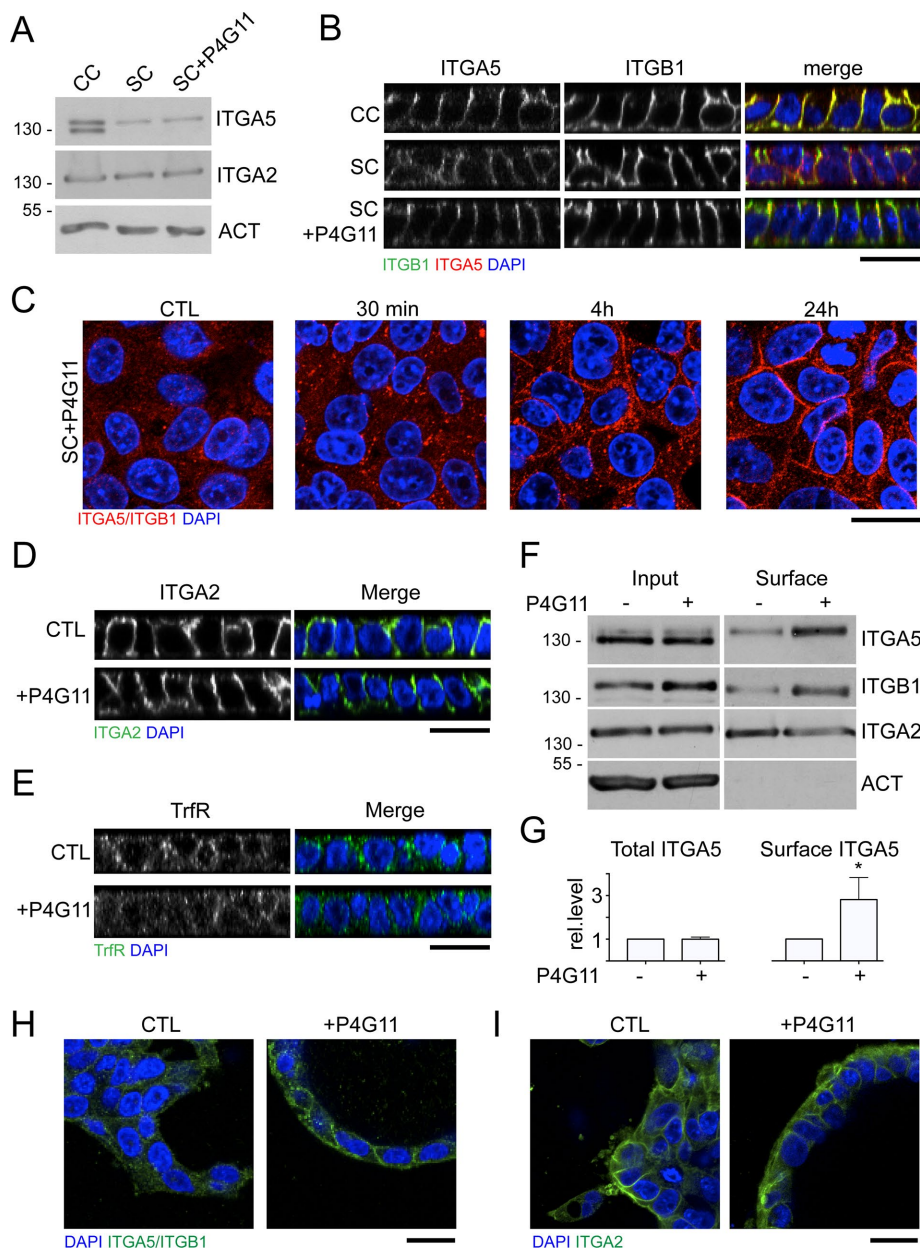


**FIGURE 5:** P4G11 selectively induces membrane localization of integrin  $\alpha 5\beta 1$ . (A) CC, SC, and SC treated with P4G11 were grown in 3D type 1 collagen as in Figure 1A. Immunoblot analysis of total levels of integrin  $\alpha 5$ , integrin  $\alpha 2$ , and actin. (B) Representative XZ-plane reconstruction of CC, SC, and SC treated with P4G11, grown on MMC-coated Transwell filters for 5 d, and treated with P4G11 on days 5–6, stained with antibodies against integrin  $\alpha 5\beta 1$  (red), integrin  $\alpha 2$  (green), and DAPI (blue). Scale bar, 20  $\mu\text{m}$ . (C) Representative confocal image of SC cells treated with P4G11 for indicated lengths of time, stained with antibody against integrin  $\alpha 5\beta 1$  (red) and DAPI (blue). Scale bar, 20  $\mu\text{m}$ . (D, E) Representative XZ-plane of SC cells grown on Transwell filters for 5 d, stained with antibodies against integrin  $\alpha 2$  (H, green), TrfR (I, green), and DAPI (blue). Scale bar, 20  $\mu\text{m}$ . (F) SC grown on Transwell filters as in B underwent cell-surface biotinylation at 4°C, followed by lysis and streptavidin (SA) pull down of biotinylated protein. Relative levels of integrin  $\alpha 5$ , integrin  $\beta 1$ , integrin  $\alpha 2$ , and actin in total and after SA pull down were analyzed in each fraction by immunoblotting. (G) Levels of integrin  $\alpha 5$  in F were quantified using ImageJ (mean  $\pm$  SEM;  $n = 3$ ). (H) Representative confocal image of SC treated with P4G11 in 3D type 1 collagen as in Figure 1A, stained with antibody against integrin  $\alpha 5\beta 1$  (green) and DAPI (blue). Scale bar, 20  $\mu\text{m}$ . (I) Representative confocal image of SC treated with P4G11 in 3D type 1 collagen, stained with an antibody against integrin  $\alpha 2$  (green) and DAPI (blue). Scale bar, 20  $\mu\text{m}$ . Asterisks signify statistical significance with  $p < 0.05$ .

To examine this further, we treated SC cells, which polarize on Transwell filters and have low levels of integrin  $\alpha 5$  on the cell surface (Figure 5F), with JBS5, a mAb that blocks integrin  $\alpha 5$  signaling by inhibiting the integrin  $\alpha 5$  and fibronectin interaction (Mould *et al.*, 1997). We grew SC cells on filters in the presence of JBS5 for 6 d. Cells were then fixed, and their organization was assessed by confocal microscopy. We found that blockade of integrin  $\alpha 5$  signaling abrogated the ability of SC cells to form a polarized monolayer and resulted in profound actin disorganization, accompanied by decreases in surface levels of E-cadherin and ZO-1 (Supplemental Figure S4, A–D). Treatment of CC in 3D with JBS5 on days 1–15 resulted in significantly fewer well-organized colonies (Supplemental Figure S4, E and F). Taken together, these data suggest that integrin  $\alpha 5$  contributes to epithelial morphogenesis in these CRC cells. Moreover, we propose that localization and activity of integrin  $\alpha 5$ , rather than simply net protein levels, mediate these effects.

#### Lateral deposition and polymerization of fibronectin is necessary and sufficient to induce epithelial polarity

Integrin  $\alpha 5$  has been shown to increase cell-cell cohesion through fibronectin deposition (Robinson *et al.*, 2004). Thus we asked whether lateral integrin  $\alpha 5$  clustering induces epithelial polarization via changes in fibronectin localization and polymerization. We treated SW480 cells cultured on MMC-coated coverglass with P4G11 for 48 h and probed for lateral ECM deposition. We found that P4G11-treated cells formed large fibronectin deposits at the cell surface (Figure 7, A–C), whereas the distribution of laminin, which is bound by integrin  $\beta 1$  paired with integrins  $\alpha 3$  and  $\alpha 6$ , was unchanged (Figure 7A). Fibronectin colocalized with lateral integrin  $\alpha 5$ , with the latter residing underneath ZO-1 (Figure 7, A and F). To determine whether the lateral fibronectin is polymerized, we performed a 1% deoxycholate (DOC) solubility assay on P4G11-treated SW480 cells, as previously described (McKeown-Longo and Mosher, 1983). Whereas levels of DOC-soluble fibronectin monomer are similar in treated and untreated cells, treatment with P4G11 leads to higher levels of DOC-insoluble fibronectin (Figure 7D). To confirm that integrin  $\alpha 5$  is responsible for the observed fibronectin deposition, we eliminated integrin  $\alpha 5$  in SW480-A5sh1 cells by administration of Dox and then treated these cells with P4G11. P4G11 no longer induced fibronectin deposition in

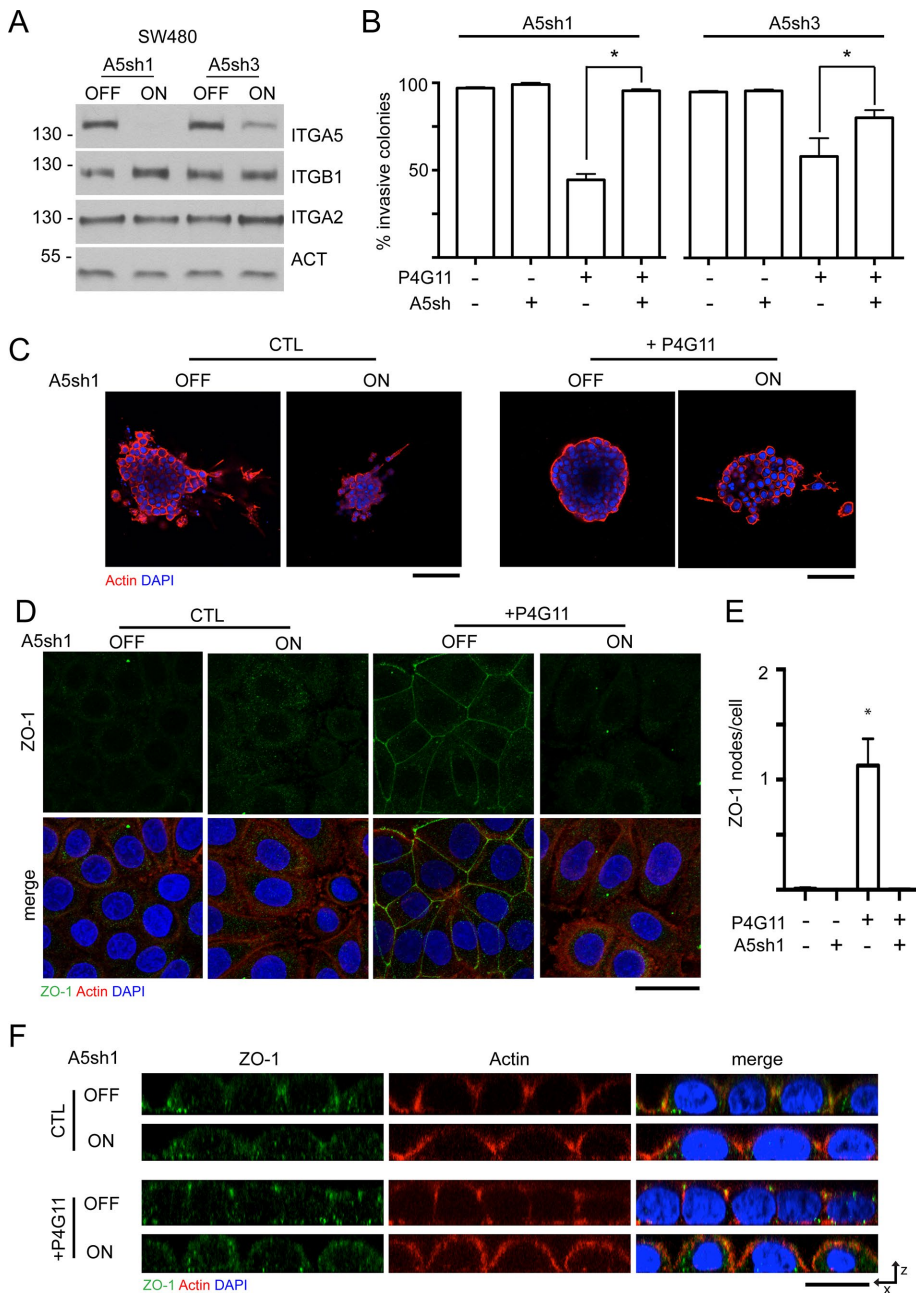


**FIGURE 6:** Integrin  $\alpha 5$  is necessary for P4G11-mediated restoration of epithelial junctions in vitro. (A) Immunoblot analysis of total levels of integrin  $\alpha 5$ , integrin  $\beta 1$ , integrin  $\alpha 2$ , and  $\beta$ -actin in SW480 cells engineered to produce anti-integrin  $\alpha 5$  shRNA in the presence (ON) or absence (OFF) of doxycycline. Two different shRNAs (A5sh1 and A5sh3) targeting different parts of the integrin  $\alpha 5$  gene were compared. (B) Quantification of the percentage of invasive SC colonies present when cells in A were grown in 3D type 1 collagen and treated with P4G11 in the presence (shA5 +) or absence (shA5 -) of anti-integrin  $\alpha 5$  shRNA. Note lack of response to P4G11 in colonies expressing anti-integrin  $\alpha 5$  shRNA (mean  $\pm$  SEM;  $>300$  colonies from three separate replicates). (C) Representative confocal image of cells in A grown in 3D type 1 collagen as in Figure 1A and treated with P4G11 in presence (ON) or absence (OFF) of anti-integrin  $\alpha 5$  shRNA (A5sh1 shown) stained with phalloidin (red) and DAPI (blue). Scale bar, 100  $\mu$ m. (D) Representative maximum intensity projections of SW480 cells grown on MMC-coated coverglass stained with phalloidin (red), DAPI (blue), and an antibody against ZO-1 (green). Scale bar, 20  $\mu$ m. (E) Quantification of number of cells exhibiting ZO-1 localization of cell-cell membranes through ImageJ analysis (see *Materials and Methods*; mean  $\pm$  SEM; more than five 20 $\times$  fields of view from three separate replicates). (F) Representative XZ-plane reconstruction of cells in A stained with antibodies against ZO-1 (green), phalloidin (red), and DAPI (blue). Scale bar, 20  $\mu$ m. Asterisks signify statistical significance with  $p < 0.05$ .

these integrin  $\alpha 5$ -knockdown cells (Figure 7E). SC cells showed a similar redistribution of fibronectin to the lateral surface after P4G11 treatment (Supplemental Figure S5C). Together these data led us to conclude that lateral clustering of integrin  $\alpha 5$  induces fibronectin polymerization.

Polymerized fibronectin has biological properties distinct from its monomeric counterpart. Thus we wanted to characterize the role of polymerized fibronectin in the restoration of apicobasolateral polarity. It has been shown that serum-derived, soluble fibronectin is necessary to initiate fibronectin polymerization (Sottile and Hocking, 2002). We found that the laterally deposited fibronectin formed by P4G11-treated SW480 cells contained both bovine and human fibronectin (Supplemental Figure S5B). To test whether serum fibronectin is required to initiate fibronectin deposition and restoration of apicobasolateral polarity, we treated SW480 cells with P4G11 in medium containing fibronectin-depleted serum. We continued to observe lateral integrin  $\alpha 5$  clustering, but fibronectin deposition and paxillin relocalization were both disrupted, as was tight junction formation. Addition of bovine fibronectin rescued fibronectin deposition and tight junction formation (Figure 8A). We next blocked fibronectin polymerization using the inhibitory peptide pUR4B paired with the control III-11C peptide, as previously described (Shi *et al.*, 2014). Concurrent treatment with P4G11 and pUR4B, but not the control peptide, abrogated the ability of P4G11 to induce fibronectin polymerization, lateral paxillin recruitment, and tight junction formation (Figure 8B). These data led us to propose a model in which lateral, integrin  $\alpha 5$ -mediated fibronectin polymerization contributes to epithelial morphogenesis (Figure 9).

If this model is correct, we expect addition of polymerized fibronectin, but not monomeric fibronectin, to recapitulate the P4G11 phenotype in the absence of antibody. We treated SW480 cells with monomeric fibronectin or polymerized superfibronectin on MMC-coated coverglass in the absence of P4G11. Treatment with polymerized superfibronectin but not monomeric fibronectin was sufficient to trigger integrin  $\alpha 5$  clustering, appearance of lateral fibronectin, and ZO-1 recruitment to tight junctions (Figure 8C). Overall these data show that polymerization of fibronectin not only is necessary but is also sufficient to drive the integrin  $\alpha 5$ -induced process leading to epithelial polarity. To assess a possible physiological role for these findings, we examined the distribution of integrin subunits and

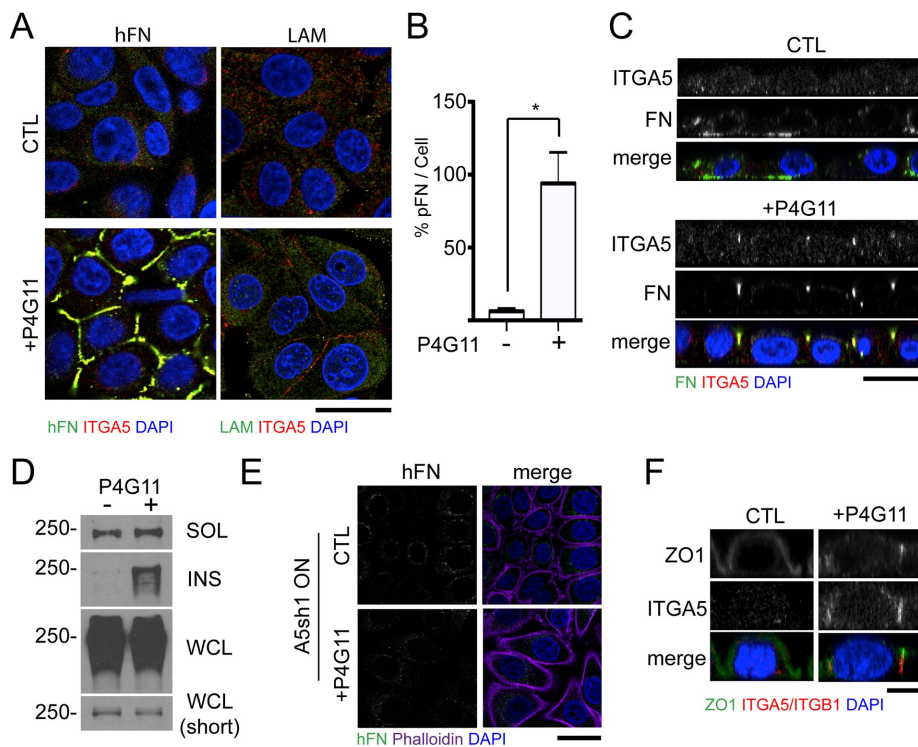


**FIGURE 7:** Integrin  $\alpha 5$  clustering leads to fibronectin polymerization and paxillin localization to the lateral surface in vitro. (A) SW480 cells were grown on MMC-coated coverglass and treated with P4G11 for 48 h. Representative confocal image of SW480 cells stained with antibodies against DAPI (blue), integrin  $\alpha 5 \beta 1$  (red), and either human fibronectin or laminin (green). Note that only fibronectin is assembled and deposited laterally in response to P4G11 treatment. Scale bar, 20  $\mu$ m. (B) Quantification of amount of fibronectin deposits per field of view normalized to cell number as in A (mean  $\pm$  SEM; more than five fields of view from three separate replicates). (C) Representative XZ-plane reconstruction of SW480 cells stained with antibodies against integrin  $\alpha 5 \beta 1$  (red), human fibronectin (green), and DAPI (blue). Scale bar, 20  $\mu$ m. (D) Analysis of fibronectin polymerization in SW480 cells grown as in A by 1% DOC solubility assay (SOL, soluble in 1% DOC; INS, insoluble in 1% DOC; WCL, whole-cell lysate), followed by immunoblotting with an antibody against fibronectin. (E) Representative confocal cross section of SW480-A5sh1 cells treated with P4G11 in the presence of Dox and stained with antibodies against human fibronectin, phalloidin (purple), and DAPI (blue). Scale bar, 10  $\mu$ m. (F) Representative XZ-plane reconstruction of cell-cell junction between SW480 cells stained with antibodies against ZO-1 (green), integrin  $\alpha 5 \beta 1$  (red), and DAPI (blue). Scale bar, 5  $\mu$ m. Asterisks signify statistical significance with  $p < 0.05$ .

fibronectin in human colon. We noted that integrin  $\alpha 5$  levels are highest at the lateral surface of terminally differentiated colonocytes, where it colocalizes with fibronectin (Figure 10). Further, we examined integrin  $\alpha 5$  localization in a small number of CRCs ( $n = 3$ ). We noted a lack of membrane integrin  $\alpha 5$  in the tumor compared with adjacent normal mucosa (Supplemental Figure S6). These findings suggest an in vivo role for lateral integrin  $\alpha 5$  in human colonic epithelial homeostasis.

## DISCUSSION

It has been appreciated that integrin signaling is required for the formation of a polarized epithelial monolayer (O'Brien *et al.*, 2001; Yu *et al.*, 2005; Chen and Krasnow, 2012). By binding to the basal ECM, integrin  $\beta 1$  is activated. This provides a cue for cell-cell junctions to be established, resulting in the development and maturation of adherens junctions and tight junctions. Recent work showed that the contribution of integrin  $\beta 1$  to apicobasolateral polarity is more complex than this simplified view (Akhtar and Streuli, 2013; Elias *et al.*, 2014). Here we discovered that integrin  $\beta 1$ -activating

mAb P4G11 is able to restore apicobasolateral polarity to disorganized and invasive CRC cells. Using P4G11 as a tool, we showed that activation of integrin  $\beta 1$  at the lateral membrane leads to clustering of integrin  $\alpha 5 / \beta 1$ . Lateral integrin  $\alpha 5$ , in turn, results in local polymerization of fibronectin. We demonstrated that inducible knockdown of integrin  $\alpha 5$  blocks the epithelial-reorganizing effect of P4G11, and addition of polymerized fibronectin is sufficient to confer this effect.

Antibodies that alter the function of integrin  $\beta 1$  have different biological effects in live-cell studies. These antibodies bind the integrin  $\beta 1$  extracellular domain and elicit conformational changes that either activate or inhibit signaling (Byron *et al.*, 2009). Each antibody has a different epitope, many of which are mapped. Recent work confirmed the existence of a conformationally inactive form of integrin  $\alpha 5 \beta 1$  and highlighted differences in receptor conformation in complex with different mAbs (Su *et al.*, 2016). Most of the work characterizing these function-altering antibodies has been related to mapping epitopes and using these to detect conformational changes in the receptor. A notable exception is work using these mAbs to track how integrin  $\beta 1$  activation alters its interaction partners and its rate of endocytosis (Humphries *et al.*, 2005; Araki *et al.*, 2009; Arjonen *et al.*, 2012). Here we provided a detailed characterization of the effects of two activating antibodies on integrin  $\beta 1$  dynamics. We confirmed previous reports that P4G11, like 12G10, is a LIBS antibody and is therefore believed to bind to and stabilize integrin  $\beta 1$  in the extended conformation (Humphries *et al.*, 2005; Araki *et al.*, 2009). Structural studies of 12G10 and TS2/16 confirmed this activating effect of 12G10 on integrin  $\beta 1$  conformation (Su *et al.*, 2016). On

the basis of our findings, we predict that P4G11 has a similar effect on the conformation of bound integrin  $\beta 1$ . Because they affect receptor conformation in similar ways, the effects of different LIBS antibodies on integrin  $\beta 1$  function are believed to be alike. However, this is not the case. Three different integrin  $\beta 1$ -activating antibodies, 12G10, TS2/16, and P4G11, have distinctly different effects on colony morphology in 3D. Further analysis of 12G10 and P4G11, which both bind high-affinity integrin  $\beta 1$ , show that P4G11 induces receptor clustering at the surface, whereas 12G10 induces receptor internalization and degradation. Of importance, we do not know whether the F(ab)' fragment retains function that is unrelated to restoration of polarity. Overall these data highlight the need for an in-depth understanding on how integrin  $\beta 1$  function-altering mAbs work in live cells. Further, our work identifies P4G11, a rarely used reagent, as a useful tool with which to study integrin  $\beta 1$  recycling dynamics and activation in epithelial cells.

Integrin  $\alpha 5$  is required for epithelialization in vivo and is sufficient to increase cell-cell cohesion in suspension in vitro (Robinson *et al.*, 2003; Koshida *et al.*, 2005; Brafman *et al.*, 2013). The cellular basis

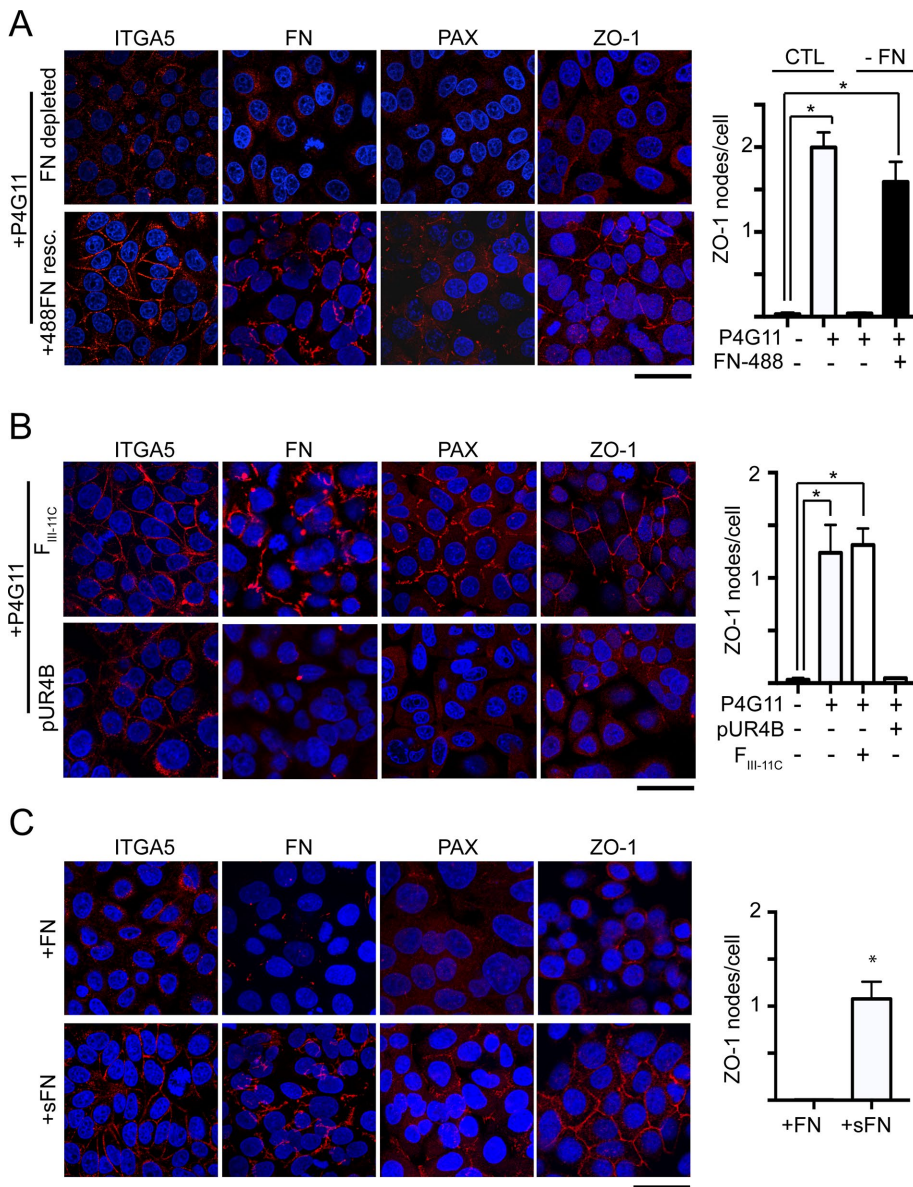


**FIGURE 8:** Fibronectin is necessary and sufficient to induce redistribution of integrin  $\alpha 5$  and paxillin to lateral membrane and induce TJ formation. SW480 cells were grown on MMC-coated coverglass and treated for 48 h as indicated and stained with antibodies against integrin  $\alpha 5$ , human fibronectin, paxillin, or ZO-1 (all shown in red) and DAPI (blue). Representative maximum intensity projections generated using confocal optical sectioning and quantification of number of cells exhibiting ZO-1 localization of cell–cell membranes through ImageJ analysis as described in Materials and Methods (mean  $\pm$  SEM; more than five 20 $\times$  fields of view from three separate replicates). Scale bars, 50  $\mu$ m. (A) Cells were grown in medium depleted of serum fibronectin and treated with P4G11 for 48 h with or without addition of 200  $\mu$ g/ml 488–bovine fibronectin. (B) SW480 cells were treated with P4G11 for 48 h in the presence of 250 nM fibronectin polymerization–blocking peptide pUR4B or control peptide F<sub>III-11C</sub>. (C) SW480 cells were treated with 20  $\mu$ g/ml polymerized superfibronectin or an equivalent amount of 488–bovine fibronectin for 48 h. Asterisks signify statistical significance with  $p < 0.05$ .

for its ability to regulate cell cohesion in the absence of a basal ECM substrate is unclear. Integrin  $\alpha 5$  has largely been studied in a variety of fibroblast-like cells, which do not exhibit robust cell–cell interactions. In these cells, integrin  $\alpha 5$  regulates multiple cellular processes, including mitosis, motility, and proliferation. Integrin  $\alpha 5$  can form a complex with ZO-1 and direct its localization, although this has not been confirmed in epithelial cells (Tuomi *et al.*, 2009; Hamalisto *et al.*, 2013). Work in Caco-2 cells showed that integrin  $\alpha 5$  expres-

sion correlates with a more epithelial phenotype and negatively regulates signaling pathways associated with the transformed phenotype (Kuwada *et al.*, 2005; Halbleib *et al.*, 2007). Our data suggest a cellular mechanism for these discrepancies. We show that retention of integrin  $\alpha 5$  at the lateral cell–cell interface restores polarity in CRC cells. We do not observe differences in integrin  $\alpha 5$  protein level during this transition, suggesting that recycling and activation dynamics are the primary drivers of this process. This effect is integrin  $\alpha 5$  specific, as we do not see differences in localization of integrin  $\alpha 2$ , another integrin  $\beta 1$  binding partner. Further, depletion of integrin  $\alpha 5$  blocks the polarity process and negatively affects the ability of cells to survive in 3D type 1 collagen in the absence of any effects on levels of integrin  $\alpha 2$  and integrin  $\beta 1$ . Inhibition of integrin  $\alpha 5$  signaling in polarizing cells blocks their ability to establish a polarized monolayer. Together these data led us to speculate that integrin  $\alpha 5$  signaling is context dependent, and lateral integrin  $\alpha 5$  signaling is required for the epithelialization process.

Interaction of fibronectin with cellular integrin  $\alpha 5$  regulates many aspects of cell behavior, including migration, growth, and differentiation (Williams *et al.*, 2008; Pimton *et al.*, 2011; Hsia *et al.*, 2014; Brennan and Hocking, 2016). It is increasingly appreciated that polymerized forms of ECM proteins elicit phenotypic changes distinct from their monomeric forms (Morla *et al.*, 1994; Pasqualini *et al.*, 1996; Sottile and Hocking, 2002). Fibronectin assembly into a fibrillar structure is an integrin-mediated process. In fibroblast cells, this occurs through integrin  $\alpha 5$  activation, binding of soluble fibronectin, and clustering. This unfolds the fibronectin molecules and allows their N-terminal ends to interact, initiating fibril assembly and polymerization (Mosher, 1993; Wu *et al.*, 1995; Sechler and Schwarzbauer, 1996). We show that integrin  $\alpha 5$  can mediate a similar process on the lateral surface of epithelial cells. As in fibroblasts, we note deposition of fibronectin in regions of integrin  $\alpha 5$  membrane localization, which, over time, results in formation of DOC-insoluble fibronectin. We also note the recruitment of paxillin, previously reported to participate in fibronectin assembly (Sechler and Schwarzbauer, 1996), to the regions of fibril deposition. There is some controversy over the ability of other RGD integrins to mediate fibronectin assembly. Our integrin  $\alpha 5$  depletion studies support the model in which integrin  $\alpha 5$  is necessary for this process. To our knowledge, this is the first time that lateral integrin  $\alpha 5$ -mediated polymerization of fibronectin has been observed in epithelial cells.

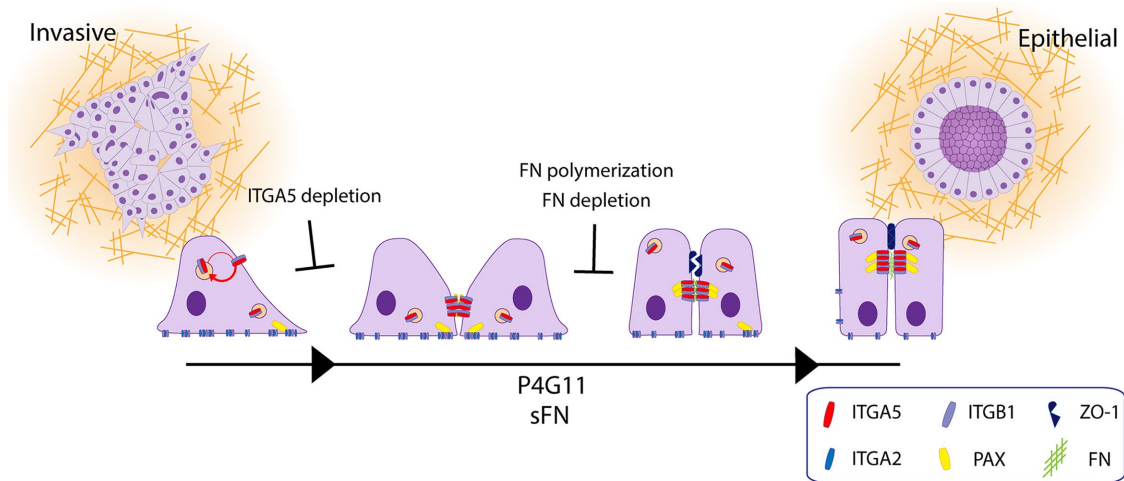


**FIGURE 9:** Model depicting the process of P4G11- and fibronectin-mediated restoration of apicobasolateral polarity. See the text for details.

Increases in intercellular fibronectin deposition positively correlate with cell–cell cohesion (Robinson *et al.*, 2004). The cell–cell adhesion proteins that contribute to this increase in adhesion have not been identified. Although these previous data were derived from nonpolarizing cells, our data support a fibronectin-mediated increase in cell–cell interaction. In intestinal cells, lateral deposition of fibronectin at cell–cell junctions has been observed *in vitro* (Quaroni *et al.*, 1978). We note that fibronectin polymerization laterally between cells alters cell morphology and restores tight junction formation and cell polarity. Polymerized fibronectin has antimetastatic effects and can cluster cell surface integrin  $\alpha 5$  (Schwartz *et al.*, 1991; Pasqualini *et al.*, 1996). Addition of polymerized superfibrinogen to disorganized cells is sufficient to induce integrin  $\alpha 5$  clustering and tight junction formation, further supporting our model. Taken together, these observations suggest a role for polymerized fibronectin in epithelial cell–cell adhesion. The dynamics of this process, as well as the proteins that mediate the increased intercellular cohesion, have yet to be characterized.

Integrins and ECM proteins are differentially expressed along the crypt–villus axis of intestinal crypts (Beaulieu *et al.*, 1991). Integrin  $\beta 1$  surface levels are higher in the proliferative progenitor compartment at the crypt base (Fujimoto *et al.*, 2002). Integrin  $\beta 1$  is required for proper intestinal organization. Deletion of integrin  $\beta 1$  in the intestinal epithelium during development resulted in intestinal epithelial cell hyperproliferation, impaired differentiation, and, ultimately, early postnatal lethality (Jones *et al.*, 2005). Intestinal epithelial cells in these knockdown mice show impaired endocytosis and a deregulation of pathways that normally regulate intestinal homeostasis. An inducible depletion of integrin  $\beta 1$  in the adult gut has not been performed (Xu *et al.*, 2014).

Little is known about the contribution of integrin  $\beta 1$ -binding  $\alpha$ -integrins to intestinal development and homeostasis. We detect a complex of integrin  $\alpha 5\beta 1$ /fibronectin at the lateral membrane of terminally differentiated colonic epithelial cells at the luminal surface. Of interest, cell–cell connections are known to be tighter at the luminal surface than at the crypt base. These data led us to propose a model in which a lateral integrin  $\alpha 5$ /fibronectin complex participates in tightening of cell–cell junctions as cells within the colonic crypt undergo terminal differentiation. Integrin  $\alpha 5$  staining was absent in

a small number of CRCs that we examined. Future studies are needed to determine whether loss of lateral integrin  $\alpha 5$  participates in cancer progression and whether retention of integrin  $\alpha 5$  at the lateral membrane can delay or even thwart cancer progression.

In summary, our results show that integrin  $\alpha 5\beta 1$  clustering at the lateral membrane can induce fibronectin polymerization, and this restores apicobasolateral polarity in invasive, disorganized CRC cells. This adds to a growing body of research supporting the view that integrin  $\beta 1$  and its associated  $\alpha$  integrins contribute much more to cell behavior than anchoring integrin  $\beta 1$  to the basal ECM.

## MATERIALS AND METHODS

### Cell culture

All cell lines were maintained in DMEM containing 10% bovine growth serum, nonessential amino acids, L-glutamine, and penicillin/streptomycin. For 3D cultures, type 1 collagen was diluted in DMEM containing 10% fetal bovine serum (FBS). Stable TET-ON anti-integrin  $\alpha 5$  shRNA expressing SW480 and SC cells were generated using the SMARTvector-inducible lentiviral shRNA construct. shRNA sequences (GATTCTCAGTGGAGTTTAA) sh1, targeting exon 1, and (AAGGGAACCTCACTTACGG) sh3, targeting exon 9, were selected by immunoblotting as having best knockdown efficiency. Cells were infected with lentivirus and selected with, and subsequently induced, using 1  $\mu\text{g}/\text{ml}$  Dox. High (top 10%) green fluorescent protein-expressing populations were fluorescently sorted. Cells were propagated in absence of Dox using DMEM containing 10% TET-free FBS. Levels of integrin  $\alpha 5$  were comparable in uninduced cells. Silencing on addition of Dox was confirmed by immunoblotting. Owing to the long half-life of integrin  $\alpha 5$ , cells were grown in Dox for at least 72 h before plating for an experiment.

### Reagents

PureCol bovine type 1 collagen was purchased from Advanced Biomatrix (San Diego, CA). All cell culture components were purchased from Hyclone Laboratories. Protein G agarose and rhodamine-phalloidin were purchased from Life Technologies. Alexa Fluor 488-conjugated fibronectin was purchased from Cytoskeleton. Fibronectin-free serum was a kind gift from Alissa Weaver. Fibronectin polymerization-blocking pUR4B and the control III-11c peptides were a kind gift from J. Sottile and were used at a final concentration of 250 nM.

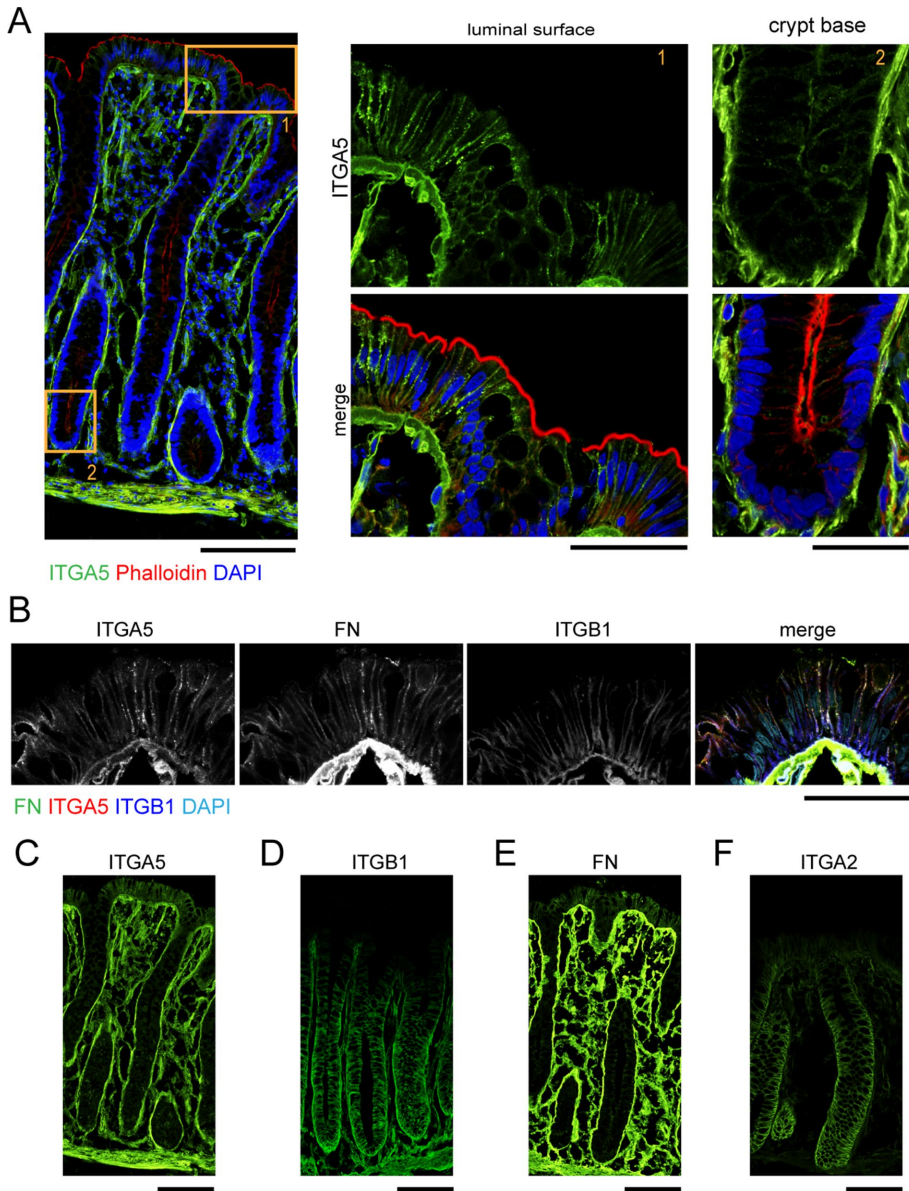


**FIGURE 10:** Integrin  $\alpha 5$  is present at the lateral surface in the terminally differentiated compartment of the normal human colon. (A) Representative confocal images of a normal human colon section stained with antibody against integrin  $\alpha 5$  (green), phalloidin (red), and DAPI (blue); scale bar, 100  $\mu\text{m}$ . High-magnification view of differentiated (1) and progenitor (2) regions of crypt. Scale bar, 50  $\mu\text{m}$ . (B) High magnification of epithelial cells at the luminal surface stained with antibodies against integrin  $\alpha 5$  (red), fibronectin (green), integrin  $\beta 1$  (blue), and DAPI (teal). (C–F) Sections of normal human colon stained with antibodies against integrin  $\alpha 5$  (C), integrin  $\beta 1$  (D), fibronectin (E), and integrin  $\alpha 2$  (F). Scale bars, 50  $\mu\text{m}$ .

### Antibodies

A1B2 and P4G11 hybridomas were purchased from the Iowa Developmental Studies Hybridoma Bank. Antibodies were produced and purified by the Vanderbilt Antibody Core Facility (VAPR). P4G11 was used at 10  $\mu\text{g}/\text{ml}$  in all studies, unless otherwise indicated. DyLight 594-conjugated P4G11 was produced by the VAPR. Monovalent P4G11 F(ab)' fragments were produced using the Ficin Digestion Kit from Millipore and conjugated to DyLight 594 by the VAPR. Total integrin  $\beta 1$  antibody P5D2, activating antibody 12G10, and 12G10–Alexa Fluor 488 were purchased from Abcam. Integrin  $\beta 1$ -activating

mAb TS2/16 and integrin  $\alpha 5$ -blocking JBS5 were purchased from ThermoFisher. Antibodies for ezrin, fibronectin, paxillin, ZO-1, integrin  $\alpha 2$ , and TrfR were purchased from Abcam. Rat monoclonal anti-integrin  $\alpha 5\beta 1$  was purchased from ThermoFisher. All secondary antibodies were purchased from Invitrogen.

### Three-dimensional type 1 collagen cultures

Briefly, assays were set up using three layers of type 1 collagen. Top and bottom layers were 2 mg/ml collagen alone, and the middle layers consisted of 2 mg/ml collagen plus cells at 5000 cells/ml in single-cell suspension. All three layers contained 400- $\mu\text{l}$  volume per well of a 12-well culture dish. Medium (400  $\mu\text{l}$ ) with or without reagents was added on top and changed every 2–3 d. Colonies were observed and counted after 14–17 d. All antibodies were used at 10  $\mu\text{g}/\text{ml}$ .

### Monomeric collagen coating

Coverglass or Transwell filters were incubated with 0.3 mg/ml type 1 collagen for 30 min and rinsed twice with phosphate-buffered saline (PBS).

### Colony counting

Colonies were counted using GelCount (Oxford Optronix) with identical acquisition and analysis settings and represented as mean from triplicates  $\pm$  SEM. For cystic and spiky morphology, counts were performed manually from three individual wells and represented as mean  $\pm$  SEM.

### Protein isolation from 3D culture for immunoblotting

To isolate cells from 3D collagen, 1 ml of collagenase solution (1 mg/ml collagenase I dissolved in complete medium) was added to one well of the 12-well plate and incubated at 37°C until gels dissolved (between 1 and 2 h). Then cells were collected by centrifugation, washed twice with PBS, and lysed in 1% Triton buffer containing protease (Complete Protease Inhibitor Cocktail Tablets from Roche).

### Immunoblotting

Cell lysates were generated from 3D collagen cultures as described. Briefly, the middle layer was removed and placed into 100  $\mu\text{l}$  of RIPA buffer for 30 min at 4°C. Sample was then centrifuged at 14,000 rpm for 10 min to get rid of solid collagen pellet. Supernatant was diluted with 4 $\times$  Laemmli buffer and 10%  $\beta$ -mercaptoethanol (BME), boiled for 5 min, and separated on a 8% SDS-PAGE reducing gel. Lysates were then transferred overnight onto a nitrocellulose membrane, blocked for 30 min in 5% milk, and incubated overnight with antibodies at 4°C. Membranes

were washed and developed with secondary horseradish peroxidase-linked antibodies. Cells grown on MMC-coated plastic or glass were lysed in sample buffer with 10% BME, briefly sonicated to shear nucleic acids, and boiled for 5 min before running on an SDS-PAGE reducing gel.

### Solubility assay in 1% DOC

For analysis of fibronectin polymerization, cells were lysed in 1% DOC (Sigma-Aldrich) as previously described. Lysates were centrifuged at  $20,000 \times g$  for 10 min. Supernatant and pellet were separated, diluted in 4 $\times$  sample buffer, and analyzed by immunoblotting.

### Immunofluorescence

**Three-dimensional immunofluorescence.** Collagen sandwich was fixed in 4% paraformaldehyde (PFA) for 30 min at room temperature. Middle layer was removed and placed into IF buffer (1% BSA, 1% Triton X-100 in PBS) overnight. Alexa Fluor 568-phalloidin and 4',6-diamidino-2-phenylindole (DAPI) were added for 4 h at 4°C before wash and confocal microscopy on Nikon A1R. For immunofluorescence, primary antibodies were added at 1:200 overnight in IF buffer. Samples were then washed, and secondary antibody was added at 1:1000 for 1 h at 4°C. Samples were washed and whole mounted onto a #1.5 glass coverslip and subsequently analyzed using confocal microscopy on a Nikon A1R LSM.

**Tissue section.** Tumor xenografts or human tissues were fixed in 4% PFA, placed overnight in 30% sucrose, and frozen in OCT compound (TissueTech). Frozen blocks were cryosectioned into 6- $\mu$ m sections, permeabilized with 1% Triton, and blocked with glycine (0.3 M, 30 min) and DAKO protein block (1 h) sequentially. Primary antibody was added overnight. Secondary antibodies from Invitrogen (Alexa Fluor linked) were added 1:1000 for 30 min. Slides were washed, mounted in Prolong (Life Technologies), and analyzed with confocal microscopy using a Nikon A1R LSM confocal microscope.

### Transmission electron microscopy

SC grown in 3D type 1 collagen for 15 d in the presence and absence of P4G11 were processed for TEM as previously described (Li *et al.*, 2017).

### ZO-1 quantification

The ImageJ angiogenesis analyzer was used to count the number of nodes in cells that had been fixed and stained for ZO-1 localization. The number of ZO-1 nodes in each field was normalized to the number of DAPI-labeled nuclei in each field, as counted by ImageJ.

### Transwell filter diffusion assay

SW480 cells were seeded on Transwell filters and allowed to attach for 24 h. Cells were treated with P4G11 for 48 h, and then the medium in the upper well was replaced with medium containing 100  $\mu$ M 70-kDa FITC-dextran. Cells were placed at 37°C, medium was collected from the bottom chamber at different time points, and total fluorescence per well was analyzed on a BioTek plate reader.

### Statistical analysis

Two-tailed, two-sample *t* tests were used to determine statistical significance.  $p < 0.05$  was considered significant. Calculations were performed using Prism for Mac and R-2.15 (64-bit for Mac).

### ACKNOWLEDGMENTS

We acknowledge the support of Vanderbilt University's Cell Imaging, Translational Pathology, and Flow Cytometry Shared Resources. We thank Janice A. Williams for help with the transmission electron microscopy, Jane Sottile for her generous gift of the pUR4B and control plasmids, and Alissa Weaver for her generous gift of fibronectin-free serum. This work was supported by National Institutes of Health Training Grant 2T32CA009582-29 to A.S. and National Cancer Institute/National Institutes of Health Grants R01CA46413 and Specialized Programs of Research Excellence P50CA95103 to R.J.C. The content is solely the responsibility of the authors and does not necessarily represent the official views of the National Institutes of Health.

### REFERENCES

- Akhtar N, Streuli CH (2013). An integrin-ILK-microtubule network orients cell polarity and lumen formation in glandular epithelium. *Nat Cell Biol* 15, 17–27.
- Araki E, Momota Y, Togo T, Tanioka M, Hozumi K, Nomizu M, Miyachi Y, Utani A (2009). Clustering of syndecan-4 and integrin beta 1 by laminin alpha 3 chain-derived peptide promotes keratinocyte migration. *Mol Biol Cell* 20, 3012–3024.
- Arjonen A, Alanko J, Veltel S, Ivaska J (2012). Distinct recycling of active and inactive beta1 integrins. *Traffic* 13, 610–625.
- Beaulieu JF, Vachon PH, Chartrand S (1991). Immunolocalization of extracellular matrix components during organogenesis in the human small intestine. *Anat Embryol (Berl)* 183, 363–369.
- Bouvard D, Pouwels J, De Franceschi N, Ivaska J (2013). Integrin inactivators: balancing cellular functions in vitro and in vivo. *Nat Rev Mol Cell Biol* 14, 430–442.
- Brafman DA, Phung C, Kumar N, Willert K (2013). Regulation of endodermal differentiation of human embryonic stem cells through integrin-ECM interactions. *Cell Death Differ* 20, 369–381.
- Brennan JR, Hocking DC (2016). Cooperative effects of fibronectin matrix assembly and initial cell-substrate adhesion strength in cellular self-assembly. *Acta Biomater* 32, 198–209.
- Byron A, Humphries JD, Askari JA, Craig SE, Mould AP, Humphries MJ (2009). Anti-integrin monoclonal antibodies. *J Cell Sci* 122, 4009–4011.
- Calderwood DA, Shattil SJ, Ginsberg MH (2000). Integrins and actin filaments: reciprocal regulation of cell adhesion and signaling. *J Biol Chem* 275, 22607–22610.
- Campbell ID, Humphries MJ (2011). Integrin structure, activation, and interactions. *Cold Spring Harb Perspect Biol* 3, a004994.
- Chen JC, Krasnow MA (2012). Integrin beta 1 suppresses multilayering of a simple epithelium. *PLoS One* 7, e52886.
- Dransfield I, Cabanas C, Craig A, Hogg N (1992). Divalent cation regulation of the function of the leukocyte integrin LFA-1. *J Cell Biol* 116, 219–226.
- Elias BC, Mathew S, Srichai MB, Palamuttam R, Bulus N, Mernaugh G, Singh AB, Sanders CR, Harris RC, Pozzi A, *et al.* (2014). The integrin beta 1 subunit regulates paracellular permeability of kidney proximal tubule cells. *J Biol Chem* 289, 8532–8544.
- Fujimoto K, Beauchamp RD, Whitehead RH (2002). Identification and isolation of candidate human colonic clonogenic cells based on cell surface integrin expression. *Gastroenterology* 123, 1941–1948.
- Halbleib JM, Saaf AM, Brown PO, Nelson WJ (2007). Transcriptional modulation of genes encoding structural characteristics of differentiating enterocytes during development of a polarized epithelium in vitro. *Mol Biol Cell* 18, 4261–4278.
- Hamalisto S, Pouwels J, de Franceschi N, Saari M, Ivarsson Y, Zimmermann P, Brech A, Stenmark H, Ivaska J (2013). A ZO-1/alpha5beta1-integrin complex regulates cytokinesis downstream of PKCepsilon in NCI-H460 cells plated on fibronectin. *PLoS One* 8, e70696.
- Hato T, Pampori N, Shattil SJ (1998). Complementary roles for receptor clustering and conformational change in the adhesive and signaling functions of integrin alpha(IIb)beta(3). *J Cell Biol* 141, 1685–1695.
- Howlett AR, Bailey N, Damsky C, Petersen OW, Bissell MJ (1995). Cellular growth and survival are mediated by beta 1 integrins in normal human breast epithelium but not in breast carcinoma. *J Cell Sci* 108, 1945–1957.
- Hsia HC, Nair MR, Corbett SA (2014). The fate of internalized alpha5 integrin is regulated by matrix-capable fibronectin. *J Surg Res* 191, 268–279.

- Humphries JD, Schofield NR, Mostafavi-Pour Z, Green LJ, Garratt AN, Mould AP, Humphries MJ (2005). Dual functionality of the anti-beta 1 integrin antibody, 12G10, exemplifies agonistic signalling from the ligand binding pocket of integrin adhesion receptors. *J Biol Chem* 280, 10234–10243.
- Jewell K, Kapronbras C, Jeevaratnam P, Dedhar S (1995). Stimulation of tyrosine phosphorylation of distinct proteins in response to antibody-mediated ligation and clustering of alpha(3) and alpha(6) Integrins. *J Cell Sci* 108, 1165–1174.
- Jones RG, Li XG, Gray PG, Kuwada SK (2005). Conditional deletion of beta 1 integrin in intestinal epithelium. *Gastroenterology* 128, A99–A99.
- Kornberg LJ, Earp HS, Turner CE, Prockop C, Juliano RL (1991). Signal transduction by integrins - increased protein tyrosine phosphorylation caused by clustering of beta-1 integrins. *Proc Natl Acad Sci USA* 88, 8392–8396.
- Koshida S, Kishimoto Y, Ustumi H, Shimizu T, Furutani-Seiki M, Kondoh H, Takada S (2005). Integrin alpha5-dependent fibronectin accumulation for maintenance of somite boundaries in zebrafish embryos. *Dev Cell* 8, 587–598.
- Kuwada SK, Kuang J, Li X (2005). Integrin alpha5/beta1 expression mediates HER-2 down-regulation in colon cancer cells. *J Biol Chem* 280, 19027–19035.
- Li C, Singh B, Graves-Deal R, Ma H, Starchenko A, Fry WH, Lu Y, Wang Y, Bogatcheva G, Khan MP, et al. (2017). Three-dimensional culture system identifies a new mode of cetuximab resistance and disease-relevant genes in colorectal cancer. *Proc Natl Acad Sci USA* 114, E2852–E2861.
- Li CX, Ma HT, Wang Y, Cao Z, Graves-Deal R, Powel AE, Starchenko A, Ayers GD, Washington MK, Kamath V, et al. (2014). Excess PLAC8 promotes an unconventional ERK2-dependent EMT in colon cancer. *J Clin Invest* 124, 2172–2187.
- McKeown-Longo PJ, Mosher DF (1983). Binding of plasma fibronectin to cell-layers of human-skin fibroblasts. *J Cell Biol* 97, 466–472.
- Morla A, Zhang Z, Ruoslahti E (1994). Superfibronectin is a functionally distinct form of fibronectin. *Nature* 367, 193–196.
- Mosher DF (1993). Assembly of fibronectin into extracellular-matrix. *Curr Opin Struct Biol* 3, 214–222.
- Mould AP, Askari JA, Aota S, Yamada KM, Irie A, Takada Y, Mardon HJ, Humphries MJ (1997). Defining the topology of integrin alpha5beta1-fibronectin interactions using inhibitory anti-alpha5 and anti-beta1 monoclonal antibodies. Evidence that the synergy sequence of fibronectin is recognized by the amino-terminal repeats of the alpha5 subunit. *J Biol Chem* 272, 17283–17292.
- O'Brien LE, Jou TS, Pollack AL, Zhang QH, Hansen SH, Yurchenco P, Mostov KE (2001). Rac1 orientates epithelial apical polarity through effects on basolateral laminin assembly. *Nat Cell Biol* 3, 831–838.
- Ojakian GK, Schwimmer R (1988). The polarized distribution of an apical cell-surface glycoprotein is maintained by interactions with the cytoskeleton of madin-darby canine kidney-cells. *J Cell Biol* 107, 2377–2387.
- Park CC, Zhang H, Pallavicini M, Gray JW, Baehner F, Park CJ, Bissell MJ (2006). Beta 1 integrin inhibitory antibody induces apoptosis of breast cancer cells, inhibits growth, and distinguishes malignant from normal phenotype in three dimensional cultures and in vivo. *Cancer Res* 66, 1526–1535.
- Pasqualini R, Bourdoulous S, Koivunen E, Woods VL, Ruoslahti E (1996). A polymeric form of fibronectin has antimetastatic effects against multiple tumor types. *Nat Med* 2, 1197–1203.
- Pimton P, Sarkar S, Sheth N, Perets A, Marcinkiewicz C, Lazarovici P, Lelkes PI (2011). Fibronectin-mediated upregulation of alpha5beta1 integrin and cell adhesion during differentiation of mouse embryonic stem cells. *Cell Adh Migr* 5, 73–82.
- Quaroni A, Isselbacher KJ, Ruoslahti E (1978). Fibronectin synthesis by epithelial crypt cells of rat small intestine. *Proc Natl Acad Sci USA* 75, 5548–5552.
- Robinson EE, Foty RA, Corbett SA (2004). Fibronectin matrix assembly regulates alpha5beta1-mediated cell cohesion. *Mol Biol Cell* 15, 973–981.
- Robinson EE, Zazzali KM, Corbett SA, Foty RA (2003). Alpha5beta1 integrin mediates strong tissue cohesion. *J Cell Sci* 116, 377–386.
- Schreider C, Peignon G, Thenet S, Chambaz J, Pincon-Raymond M (2002). Integrin-mediated functional polarization of Caco-2 cells through E-cadherin-actin complexes. *J Cell Sci* 115, 543–552.
- Schwartz MA, Lechene C, Ingber DE (1991). Insoluble fibronectin activates the Na/H antiporter by clustering and immobilizing integrin alpha 5 beta 1, independent of cell shape. *Proc Natl Acad Sci USA* 88, 7849–7853.
- Sechler JL, Schwarzbauer JE (1996). Coordinated regulation of fibronectin fibril assembly and actin stress fiber formation. *Cell Adhes Commun* 4, 413–424.
- Shi F, Long XC, Hendershot A, Miano JM, Sottile J (2014). Fibronectin matrix polymerization regulates smooth muscle cell phenotype through a rac1 dependent mechanism. *PLoS One* 9, e94988.
- Sottile J, Hocking DC (2002). Fibronectin polymerization regulates the composition and stability of extracellular matrix fibrils and cell-matrix adhesions. *Mol Biol Cell* 13, 3546–3559.
- Stallmach A, von Lampe B, Matthes H, Bornhoft G, Riecken EO (1992). Diminished expression of integrin adhesion molecules on human colonic epithelial cells during the benign to malign tumour transformation. *Gut* 33, 342–346.
- Su Y, Xia W, Li J, Walz T, Humphries MJ, Vestweber D, Cabanas C, Lu C, Springer TA (2016). Relating conformation to function in integrin alpha-5beta1. *Proc Natl Acad Sci USA* 113, E3872–E3881.
- Tuomi S, Mai A, Nevo J, Laine JO, Vilkki V, Ohman TJ, Gahmberg CG, Parker PJ, Ivaska J (2009). PKCepsilon regulation of an alpha5 integrin-ZO-1 complex controls lamellae formation in migrating cancer cells. *Sci Signal* 2, ra32.
- Williams CM, Engler AJ, Slone RD, Galante LL, Schwarzbauer JE (2008). Fibronectin expression modulates mammary epithelial cell proliferation during acinar differentiation. *Cancer Res* 68, 3185–3192.
- Wu CY, Keivens VM, Otoole TE, McDonald JA, Ginsberg MH (1995). Integrin activation and cytoskeletal interaction are essential for the assembly of a fibronectin matrix. *Cell* 83, 715–724.
- Xu C, Li X, Topham MK, Kuwada SK (2014). Regulation of sonic hedgehog expression by integrin beta1 and epidermal growth factor receptor in intestinal epithelium. *IUBMB Life* 66, 694–703.
- Yeaman C, Grindstaff KK, Nelson WJ (1999). New perspectives on mechanisms involved in generating epithelial cell polarity. *Physiol Rev* 79, 73–98.
- Yu W, Datta A, Leroy P, O'Brien LE, Mak G, Jou TS, Matlin KS, Mostov KE, Zegers MM (2005). Beta1-integrin orients epithelial polarity via Rac1 and laminin. *Mol Biol Cell* 16, 433–445.